Haverford College

Haverford Scholarship

2011

The Morphology of Galaxies in the Baryon Oscillation Spectroscopic Survey

Karen Masters
Haverford College, klmasters@haverford.edu

Claudia Maraston

Robert C. Nichol

Daniel Thomas

Repository Citation

The morphology of galaxies in the Baryon Oscillation Spectroscopic Survey

Karen L. Masters,[1,2][*] Claudia Maraston,[1] Robert C. Nichol,[1,2] Daniel Thomas,[1,2]
Alessandra Beifiori,[1] Kevin Bundy,[3] Edward M. Edmondson,[1] Tim D. Higgs,[1]
Alexie Leauthaud,[4,5] Rachel Mandelbaum,[6] Janine Pforr,[1] Ashley J. Ross,[1]
Nicholas P. Ross,[4] Donald P. Schneider,[7] Ramin Skibba,[8] Jeremy Tinker,[9]
Rita Tojeiro,[1] David A. Wake,[10] Jon Brinkmann[11] and Benjamin A. Weaver[9]

[1]*Institute for Cosmology and Gravitation, University of Portsmouth, Portsmouth PO1 3FX*
[2]*SEPnet, South East Physics Network (www.sepnet.ac.uk)*
[3]*Department of Astronomy, University of California, Berkeley, CA 94705, USA*
[4]*Lawrence Berkeley National Lab, 1 Cyclotron Road, Berkeley, CA 94720, USA*
[5]*Berkeley Center for Cosmological Physics, University of California, Berkeley, CA 94720, USA*
[6]*Department of Astrophysical Sciences, Princeton University, Peyton Hall, Princeton, NJ 08544, USA*
[7]*Department of Astronomy and Astrophysics, The Pennsylvania State University, 525 Davey Lab, University Park, PA 16802, USA*
[8]*Steward Observatory, University of Arizona, 933 N. Cherry Avenue, Tucson, AZ 85721, USA*
[9]*Center for Cosmology and Particle Physics, New York University, New York, NY 10003, USA*
[10]*Department of Astronomy, Yale University, New Haven, CT 06520, USA*
[11]*Apache Point Observatory, Apache Point Road, PO Box 59, Sunspot, NM 88349, USA*

ABSTRACT

We study the morphology and size of the luminous and massive galaxies at $0.3 < z < 0.7$ targeted in the Baryon Oscillation Spectroscopic Survey (BOSS) using publicly available *Hubble Space Telescope* (*HST*) imaging, and catalogues, from the COSMic Origins Survey (COSMOS). Our sample (240 objects) provides a unique opportunity to check the visual morphology of these galaxies which were targeted based solely on stellar population modelling. We find that the majority of BOSS galaxies (74 ± 6 per cent) possess an early-type morphology (elliptical or lenticular), while the remainder have a late-type (spiral disc) morphology. This is as expected from the goals of the BOSS target selection which aimed to predominantly select slowly evolving galaxies, for use as cosmological probes, while still obtaining a fair fraction of actively star-forming galaxies for galaxy evolution studies. We show that a colour cut of $(g - i) > 2.35$ is able to select a sub-sample of BOSS galaxies with ≥ 90 per cent early-type morphology and thus more comparable to the earlier Luminous Red Galaxy (LRG) samples of Sloan Digital Sky Survey (SDSS)-I/II. The remaining $\simeq 10$ per cent of galaxies above this $(g - i)$ cut have a late-type morphology and may be analogous to the 'passive spirals' found at lower redshift. We find that 23 ± 4 per cent of the early-type BOSS galaxies are unresolved multiple systems in the SDSS imaging. We estimate that at least 50 per cent of these multiples are likely real associations and not projection effects and may represent a significant 'dry merger' fraction. We study the SDSS pipeline sizes of BOSS galaxies which we find to be systematically larger (by 40 per cent) than those measured from *HST* images, and provide a statistical correction for the difference. These details of the BOSS galaxies will help users of the BOSS data fine-tune their selection criteria, dependent on their science applications. For example, the main goal of BOSS is to measure the cosmic distance scale and expansion rate of the Universe to per cent level precision – a point where systematic effects due to the details of target selection may become important.

Key words: surveys – galaxies: elliptical and lenticular, cD – galaxies: photometry – galaxies: spiral – cosmology: observations.

[*]E-mail: karen.masters@port.ac.uk

© 2011 The Authors
Monthly Notices of the Royal Astronomical Society © 2011 RAS

1 INTRODUCTION

The Baryon Oscillation Spectroscopic Survey (BOSS) is one of the four surveys being carried out as part of the Sloan Digital Sky Survey III (SDSS-III; Eisenstein et al. 2011). The main goal of the BOSS is to measure the cosmic distance scale and expansion rate of the Universe with per cent level precision at $z < 0.7$ and $z \sim 2.5$ using the Baryon Acoustic Oscillation (BAO) scale. To achieve this goal, BOSS is performing a redshift survey of 1.5 million massive luminous galaxies (between $0.3 < z < 0.7$) and 150 000 quasars at $z > 2.5$ selected from the SDSS imaging data published as part of Data Release Eight (DR8; Aihara et al. 2011).

Previous cosmological surveys of distant luminous galaxies have focused on the reddest galaxies because they are efficient tracers of the underlying dark matter distribution, e.g. Luminous Red Galaxies (LRGs; Eisenstein et al. 2001; Cannon et al. 2006). However, BOSS is now including bluer galaxies than these previous samples partly to increase the sky density of sources observed (to improve the BAO measurements), as well as to sample intrinsically bluer galaxies to provide a more representative census of the galaxy population for comparison with models of galaxy evolution (e.g. Kauffmann, White & Guiderdoni 1993).

With the goal of per cent level precision on the cosmological parameters, BOSS is entering the regime where the details of galaxy evolution, and sample selection, play an important role in understanding the systematic errors associated with accurate measurements of the clustering of galaxies on large scales. Different types of galaxies populate their dark matter haloes differently (e.g. Hogg et al. 2003; Zehavi et al. 2005; Ross & Brunner 2009), and especially evolve on different time-scales, so a detailed understanding of the galaxy types in the BOSS sample is important both for cosmology and for studies of galaxy evolution.

Galaxies are selected for inclusion in BOSS (and many other modern surveys) using stellar population models which predict the expected colours as a function of the galaxy star formation history, dust content and redshift. This method is effective as the stellar evolutionary status of a galaxy imprints onto its spectral energy distribution, hence colours, with the well-known effect that galaxies dominated by old stars, or more generally having a small scatter in age – are redder than galaxies hosting star formation. To a large extent this distinction is mirrored in the galaxy morphology, with older and redder galaxies typically having early-type morphologies, while star-forming galaxies usually possess discs. However, since a galaxy's morphology is also affected by gas accretion and merging histories which affect the dynamics of the stars, the colour and morphology of a galaxy can become decoupled.

In recent years, there has been a resurgence of interest in the morphology of galaxies, especially at low redshift. For example, Schawinski et al. (2007) and Thomas et al. (2010) constructed a sample of 50 000 visually inspected early-type galaxies from SDSS, and showed that morphology was an important factor in the interpretation of the transition region between the 'blue cloud' (late-type galaxies) and the 'red sequence' (early-type galaxies). These studies discovered and discussed so-called 'blue ellipticals', i.e. galaxies with an elliptical morphology and blue colours (also confirmed by Schawinski et al. 2009; Kannappan, Guie & Baker 2009). The Galaxy Zoo project (Lintott et al. 2008), with the help of citizen scientists, have now provided visual classifications for all galaxies in the original ($z < 0.3$) SDSS-I/II data (Lintott et al. 2011). This work has confirmed the strong correlation between colour and morphology of galaxies, but in addition highlighted objects in which the colour and morphology have become decoupled, such as the

blue ellipticals described above, and also a population of 'red spirals' (Bamford et al. 2009; Masters et al. 2010b), which have also been found elsewhere (e.g. Wolf et al. 2009; Bundy et al. 2010) and represent a significant fraction of the massive spiral population, as well as possibly an important evolutionary stepping stone for all massive late-types moving to the red sequence. Moreover, such work has re-defined the classic morphology–density relation (Dressler 1980) at low redshift as predominantly a colour–density relation, i.e. at a fixed galaxy colour, there is a weak morphology–density relationship, while at a fixed morphology, there remains a significant range of colours with density (see Blanton et al. 2005; Ball, Loveday & Brunner 2008; Bamford et al. 2009; Skibba et al. 2009).

In this paper we shall study the visual morphology, and catalogued sizes, of galaxies in the BOSS which have been targeted using colours predicted by population models. We shall accomplish the double aim of checking the effectiveness of a purely colour-based selection in targeting mostly passive early-type galaxies as well as determining the relation between colour and morphology at these redshifts. With a median seeing of 1.1 arcsec for the SDSS DR8 imaging data, the BOSS target galaxies are barely resolved (see Figs 2, 3 and 5) thus making it difficult to obtain reliable visual morphologies or sizes from these data. Therefore, higher angular resolution (and deeper) imaging is needed to determine the detailed shapes of BOSS galaxies, and the best facility currently available for studying such high-redshift galaxy populations is the *Hubble Space Telescope* (*HST*).

We construct a sample of BOSS targets detected in the publicly available *HST* imaging of the COSMic Origins Survey (COSMOS; Scoville et al. 2007). Although small (240 objects), such an unbiased match between COSMOS and BOSS provides an important sample of objects for statistical studies and is unlikely to grow in size or depth over the next few years.

Where appropriate, we assume a cosmological model of a flat, Λcold dark matter Universe with $H_0 = 70$ km s^{-1} Mpc^{-1} and $\Omega_M = 0.3$ consistent with recent *Wilkinson Microwave Anisotropy Probe* observations (Komatsu et al. 2011).

2 SAMPLE AND DATA

The SDSS-III DR8 imaging data cover 15 000 deg^2 of high galactic latitude sky comprising the SDSS-I/II Legacy survey and 3000 deg^2 of new imaging concentrated in the Southern Hemisphere (York et al. 2000; Aihara et al. 2011). Images in five filters (*ugriz*; Fukugita et al. 1996) are obtained with a CCD camera (Gunn et al. 1998) mounted on the SDSS telescope (Gunn et al. 2006).

Spectroscopic targets for BOSS are selected from the high Galactic latitude regions of this imaging (around 10 000 deg^2 in total) using colour cuts designed to select luminous, massive galaxies with an approximately uniform distribution in stellar mass over the redshift range $0.3 < z < 0.7$. The details of target selection are given in Eisenstein et al. (2011) and summarized in Section 2.3. The BOSS galaxy sample is designed to have a total angular source density of approximately 150 galaxies deg^{-2} which is an order of magnitude greater than the SDSS-I/II LRG sample.

2.1 COSMOS *HST* imaging

COSMOS is the largest *HST* survey yet undertaken and was specifically designed to survey all types of galaxy environments at $z > 0.5$ (Scoville et al. 2007). The *HST* imaging for COSMOS
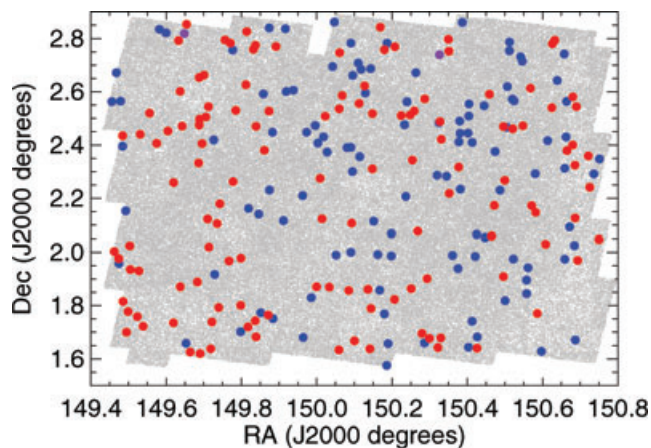
Figure 1. The sky distribution of BOSS target galaxies in the COSMOS field is shown as coloured points overplotted on the positions of all galaxies detected by COSMOS (small grey points). We identify BOSS targets by their sub-sample (see Section 2.3); CMASS objects are shown in red, while LOZ objects are shown in blue. Two of the targets fit both target criteria and are shown as purple.

(Koekemoer et al. 2007; Leauthaud et al. 2007) is publicly available[1] over a 1.64 deg^2 field centred at $\alpha = 10^h$, $\delta = 2°.2$ (J2000). The COSMOS field is covered by the SDSS-I/II Legacy imaging data and in total 240 BOSS targets are found in common between the two sets of images, consistent with the expected source density of BOSS targets (i.e. 240 targets over 1.68 deg^2 = 143 galaxies deg^{-2}). This COSMOS-BOSS sample can be considered largely representative of the entire BOSS galaxy sample, particularly in the higher redshift CMASS sub-sample (see Section 2.3), but we note that in the lower redshift (LOZ) subset ($0.2 < z < 0.4$), the presence of a significant overdensity in the COSMOS field at $z = 0.35$ (e.g. Kovač et al. 2010) may bias the morphological mix towards red, early-types through the morphology–density relation.

We show the sky distribution of these 240 BOSS targets compared to all COSMOS identified galaxies in Fig. 1. For these 240 BOSS targets, we have visually inspected images taken by the Advanced Camera for Surveys (ACS) instrument on *HST* in the *I*-band (*F814W*) filter, which at the typical redshift for BOSS corresponds to a rest-frame *V*-band filter. We also inspect *I*- and *V*-band colour composite images provided by Griffith et al. (in preparation)[2] and a different set of colour composite images made for the Galaxy Zoo: Hubble project (Lintott et al., in preparation).

We note that ACS images of other BOSS galaxies are available in the *HST* public archive in images taken for other observations. A preliminary search of the *HST* ACS public archive finds 795 images to the same depth as the COSMOS data in the *F814W* filter. Of these, only 563 were unique (i.e. the centres of the pointings are separated by more than 10 arcsec), and 398 of these 563 images are within the approximate SDSS-III BOSS imaging area. This is less than the 567 ACS images which make up COSMOS, and is roughly 70 per cent of the area of COSMOS so would add a likely ≃170 more galaxies to our comparison sample (assuming the same surface density of BOSS galaxies). While this figure could increase the sample size of our study, we note that these additional ACS fields, and associated galaxies, could be potentially biased in their morphological mix, e.g., if found in *HST* imaging of the cores of groups and clusters of

galaxies, whereas the COSMOS field would specifically avoid such bias. We also make use of the publicly available Zurich Estimator of Structural Types (ZEST) measurements (Scarlata et al. 2007) for our BOSS galaxies in COSMOS and such measurements have not been made for the entire *HST* archive. Hence, we decide to rely only on BOSS galaxies imaged by *HST* in the COSMOS area.

2.2 BOSS imaging and spectra

Throughout this paper, we use the SDSS-III DR8 pipeline photometric measurements as described in Aihara et al. (2011). Information on the SDSS pipeline and algorithms is also given in Stoughton et al. (2002).

For the colours of BOSS galaxies, we use the model magnitudes. In the SDSS pipeline (Stoughton et al. 2002), both a de Vaucouleurs and an exponential profile fit is performed on each galaxy, and the best-fitting model is a linear combination of the two profiles. Model magnitudes are calculated using the profile shape fit in *r* band and applied to each of the five SDSS bands (allowing for a variable amplitude). For apparent luminosities, we use cmodel magnitudes where the model is fit individually in each SDSS band. All magnitudes are corrected for Galactic extinction using reddening estimates from Schlegel, Finkbeiner & Davis (1998).

For SDSS-measured galaxy sizes, we use the effective radius from the de Vaucouleur fit. This is a seeing-corrected quantity, albeit with some approximations made, so seeing may have a residual effect as we will discuss further in Section 4, and especially because the typical sizes of BOSS galaxies are comparable to the size of the seeing disc.

The SDSS seeing in the COSMOS field is typical for the whole DR8 imaging, e.g. the median seeing for the whole SDSS is 1.08 arcsec with an interquartile range of 0.95–1.22 arcsec (Ross et al. 2011).[3] The median seeing for our subset of BOSS targets in COSMOS is 1.10 arcsec, with an interquartile range of 1.02–1.16 arcsec (we are quoting the parameter PSF_FWHM in *i* band from DR8).

An important caveat to this work is that the SDSS imaging in the COSMOS field has a higher sky noise level than most of the other DR8 imaging. The median sky noise level in the whole DR8 is 20.27 mag (Ross et al. 2011),[4] with an upper quartile of 20.11 mag. Almost all (97 per cent) of the BOSS targets in the COSMOS imaging have SDSS sky noise values in this upper quartile, which of course translates to noisier photometry, and shallower images than are typical for DR8. This may have an effect, in particular, on the SDSS measured sizes.

BOSS spectra were taken for 171 of the BOSS galaxy targets on 2011 March 10 (note that the entire COSMOS area fits within a single SDSS plate). These observations resulted in 166 BOSS galaxy redshifts. The observations which did not result in galaxy redshifts are made up of two spectra which had unreliable fits, or zwarning = 4; and three spectra of stars in our Galaxy. An additional 58 of the targets in our sample had redshift measurements which were taken as part of the SDSSI/II program. The remaining

---

[1] See http://irsa.ipac.caltech.edu

[2] http://www.ugastro.berkeley.edu/~rgriffit/Morphologies/

[3] The improvement in seeing over previous SDSS imaging releases is due to the large fraction of repeat images that have been taken. In such cases, the best seeing is selected for release, thus reducing the median seeing level significantly over earlier data releases.

[4] Ross et al. (2011) report this value expressed in 'nanomaggies', which are a linear unit of flux used in the SDSS collaboration. We use the conversion from a flux, *f*, in nanomaggies, to *m* in magnitudes of $m = 22.5\,\text{mag} - 2.5\log f$.

11 targets could not be observed due to problems with fibre collisions. In total this adds up to 224 of the BOSS targets (93 per cent) having reliable galaxy redshifts. Where appropriate, we use the redshift measurement for these galaxies, but do not use any additional information from the BOSS (or SDSS) spectra. We defer such an analysis for future work.

2.3 BOSS target selection

The BOSS galaxy target selection is based on colour and apparent magnitude cuts defined in the observed-frame g, r, i photometry which have been derived via population synthesis models. It also includes cuts based on point spread function (PSF) magnitudes which are used to reduce stellar contamination. The exact cuts are given in Eisenstein et al. (2011). For the scope of this paper, it suffices to recall that the BOSS target selections are split into two sub-samples which are aimed at selecting galaxies in the different redshift ranges of BOSS, namely: (1) a Low Redshift Sample (LOZ), aimed at selecting luminous massive galaxies at $0.2 < z < 0.4$ (see the area below the dashed line in Fig. 4); and (2) a higher redshift Constant Mass Sample (CMASS), selecting luminous and massive galaxies at $z > 0.4$ (area above the dashed line in Fig. 4). Note that the CMASS, high-z cut is a new BOSS cut, while the LOZ cut is similar to the original LRG Cut I selection from SDSS-I/II (Eisenstein et al. 2001).

The BOSS target selection cuts are based on the expected track of a passively evolving, constant stellar mass galaxy based on a population model for luminous red galaxies by Maraston et al. (2009). As has been discussed previously in both Eisenstein et al. (2011) and White et al. (2011), the CMASS colour selection closely tracks the redshifted colours of luminous and massive galaxies at $z \simeq 0.5$, while the (colour-dependent) i-band magnitude constraint in CMASS is aimed at selecting objects with $M_\star \simeq 10^{11}\,\mathrm{M}_\odot$, independent of their intrinsic rest-frame colours. Fig. 1 of White et al. (2011) demonstrates that this set of cuts successfully isolates galaxies at $z > 0.4$.

What is most relevant to our study is that: (i) the main colour cut for CMASS [the selection of $d_\perp = (r - i) - (g - r)/8.0 > 0.55$] is basically a selection on the observed-frame colour $(r - i)$ (i.e. the line is almost horizontal in Fig. 4). All galaxies in the redshift range of CMASS ($0.4 < z < 0.7$) have their 4000 Å break feature somewhere in the r band since at $z = 0.4$ the break is exactly between g and r at 5600 Å, and at $z = 0.75$ it moves into i band (at 7000 Å). This means that all galaxies at these redshifts are red in observed-frame $(r - i)$, regardless of the stellar content; (ii) no

strong cut was made in the observed-frame $(g - r)$, which would select approximately in intrinsic $(u - g)$ colour at these redshifts – a colour which is very sensitive to stellar content; (iii) an (slightly colour-dependent) i-band magnitude cut is applied to require that (only) massive galaxies are selected.

The stellar population model based target selection for BOSS described above implies that we should find within the sample mostly early-type galaxies, since this type of galaxy dominates the massive galaxy population. But, given the absence of a red colour cut in $(g - r)$, massive blue galaxies could also be found. We shall see in the next section (Fig. 4) that the real morphologies of the BOSS galaxies in our sample reflect well this expectation.

3 VISUAL MORPHOLOGY

We visually inspected both the COSMOS and SDSS images of all 240 BOSS target galaxies in the COSMOS area. The COSMOS images were used to first classify galaxies as either 'early' or 'late-type' morphology. We then further separated these broad classes into possibly lenticular (S0) early-type galaxies, disturbed galaxies and/or multiple systems (including multiple cores). For the late-type galaxies, we also recorded if the galaxy was viewed as an 'edge-on' disc or possessed a bar through the middle of the galaxy.

Table 1 shows the morphological mix of our sample, and we present all of our visual classifications in Appendix A. We find that the majority of BOSS galaxies in our COSMOS sample are early-type galaxies [74 ± 6 per cent; we quote the Poisson error on fractions throughout, but note that this is strictly only valid for large sample sizes and fractions close to neither 0 per cent nor 100 per cent. The error we quote will therefore be an underestimate of the true confidence region particularly for the small fractions and subsets; see Cameron (2011) for more details], but there is a substantial fraction of late-type galaxies present (24 ± 3 per cent). Representative images from each morphological class of object are provided in Fig. 2 for the CMASS sample and in Fig. 3 for the LOZ sample, and all 240 galaxies are available for inspection at http://icg.port.ac.uk/~mastersk/BOSSmorphologies/ which shows both the SDSS gri colour composites alongside the COSMOS *HST I* band and colour composite images.

3.1 Morphology and colour

BOSS target galaxies in the COSMOS field are shown in Fig. 4 as a function of their observed-frame $(g - r)$ and $(r - i)$ SDSS

Table 1. Visual morphology of BOSS galaxies in the COSMOS imaging.

Type	All BOSS	CMASS	LOZ	$(g - i) > 2.35$	CMASS $(g - i) > 2.35$
All objects	240	129	113	135	91
Early-types	178 (74 per cent)	91 (71 per cent)	88 (78 per cent)	122 (90 per cent)	83 (91 per cent)
Lenticular	34 (19 per cent)	15 (16 per cent)	19 (22 per cent)	20 (16 per cent)	12 (14 per cent)
Multiple	40 (23 per cent)	21 (23 per cent)	20 (23 per cent)	27 (22 per cent)	19 (23 per cent)
Disturbed	26 (15 per cent)	14 (15 per cent)	12 (14 per cent)	17 (14 per cent)	12 (14 per cent)
Late-types	58 (24 per cent)	34 (26 per cent)	25 (22 per cent)	13 (10 per cent)	8 (9 per cent)
Barred	11 (28 per cent)	8 (29 per cent)	4 (33 per cent)	4 (57 per cent)	4 (57 per cent)
Edge	18 (31 per cent)	6 (18 per cent)	12 (48 per cent)	6 (46 per cent)	1 (13 per cent)
Multiple	6 (10 per cent)	5 (15 per cent)	2 (8 per cent)	2 (15 per cent)	2 (25 per cent)
Disturbed	13 (22 per cent)	11 (32 per cent)	3 (12 per cent)	4 (31 per cent)	4 (50 per cent)
Stars	4 (2 per cent)	4 (2 per cent)	-	-	-
Multiple	2	2	-	-	-
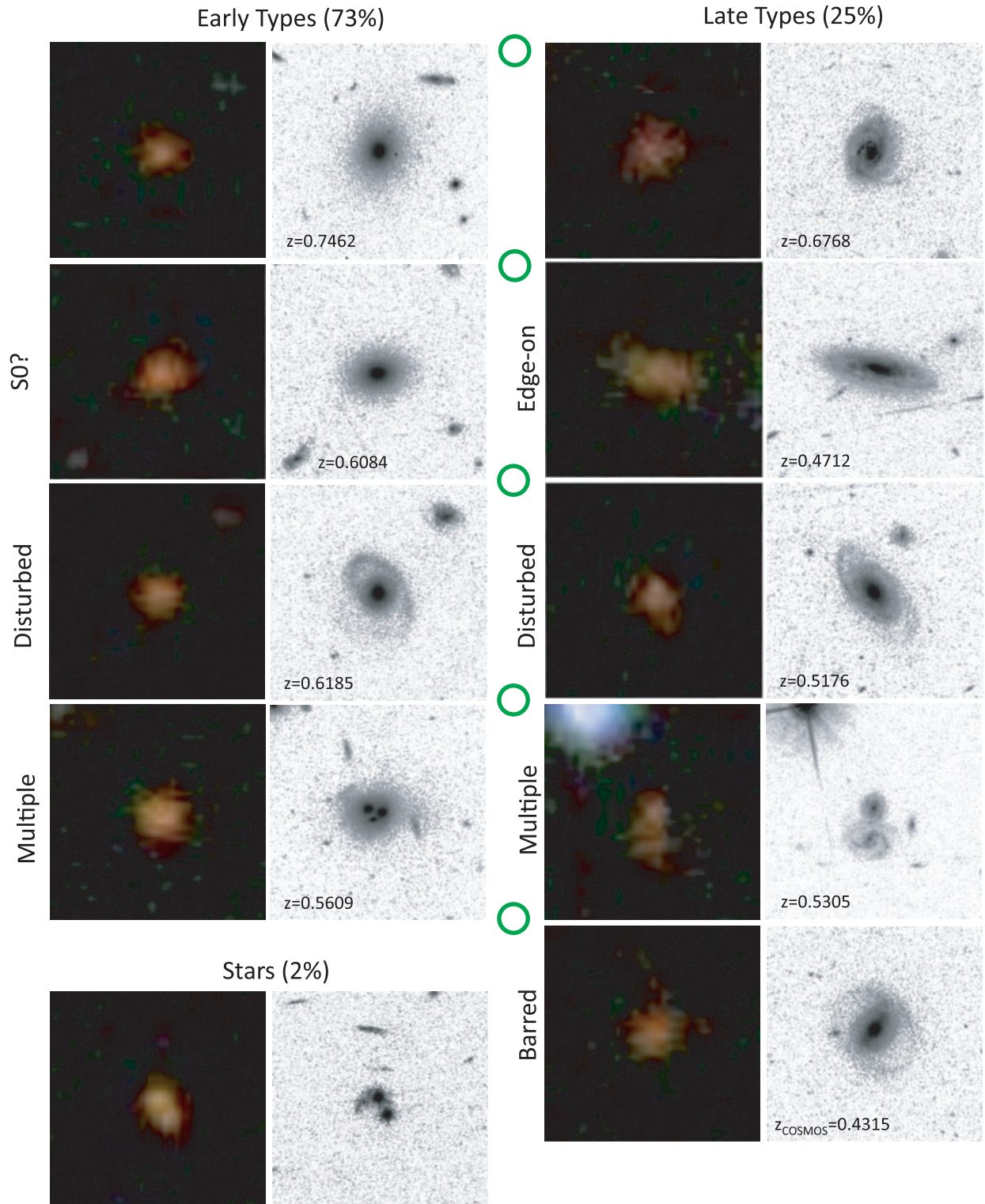
Figure 2. Examples of SDSS composite colour *gri* images and ACS *I*-band images (shown as black on white) for BOSS CMASS galaxies with different morphological types. Shown are 10 examples out of a total sample of 129 objects. All images are 15 arcsec², and the BOSS 2 arcsec diameter fibre is illustrated by a green circle. The redshifts of these objects are shown in the figure. The barred late-type was not observed by BOSS due to fibre collisions, but has a redshift from *z*COSMOS (Lilly et al. 2007). The double point source system has also been observed spectroscopically by BOSS and is confirmed to be made up of stars in our Galaxy (i.e. $z = 0$).
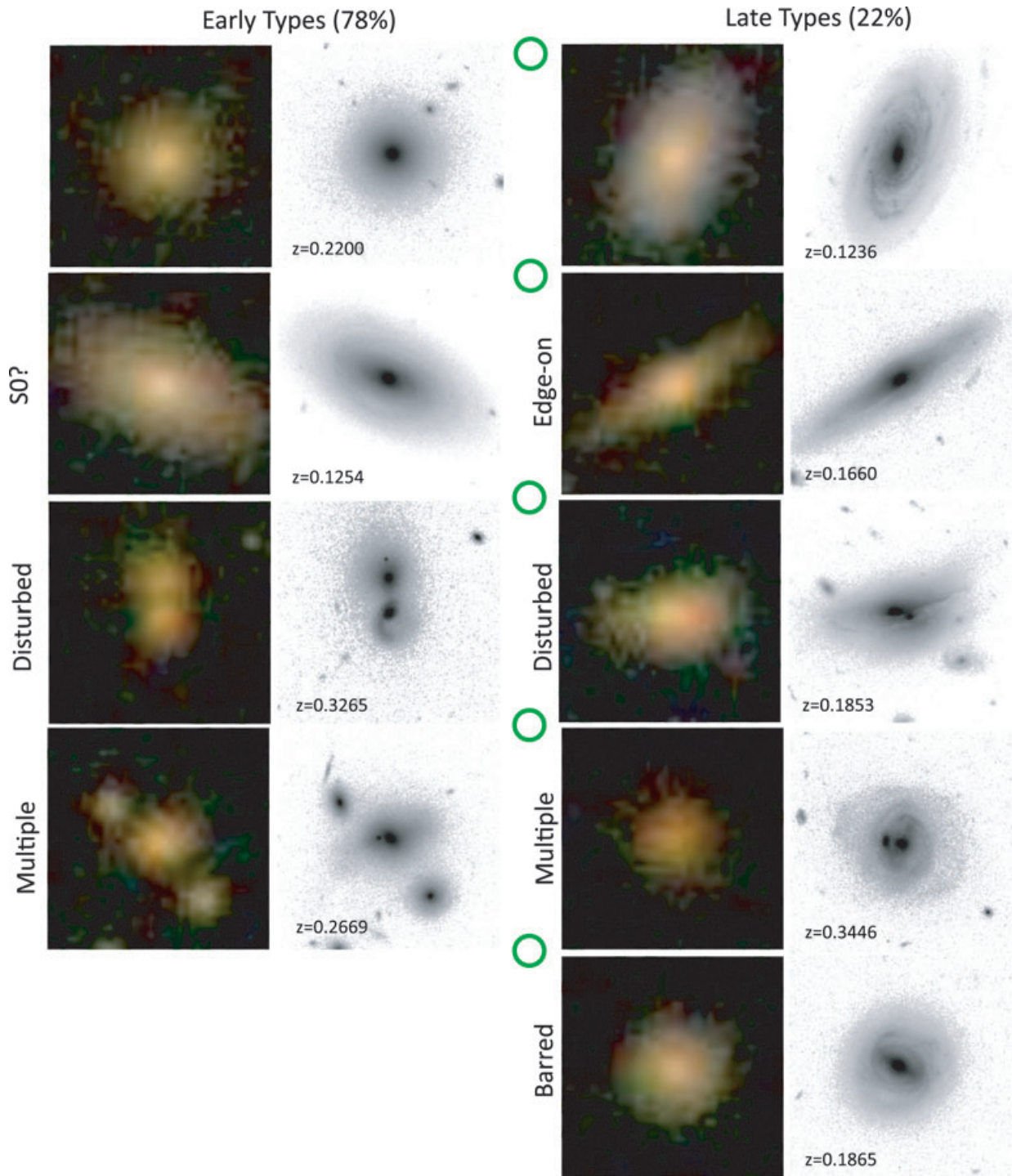
Figure 3. As with Fig. 2 but for the BOSS LOZ sample which has a total of 113 objects (and no point sources). The redshifts of these objects mostly come from SDSS-I/II observations). We note that the multiple late-type galaxy also makes the colour cuts of the BOSS CMASS sample.

colours.[5] The symbols indicate the basic visual morphology of the galaxies, while the dashed diagonal line is the $d_\perp$ limit of the CMASS sample, i.e. galaxies above this line are in the CMASS sub-sample and should have redshifts larger than $z = 0.4$.

We see that the majority of objects both above and below the CMASS cut have an early-type morphology (shown as red circles) and that late-type galaxies (blue spiral symbols) in BOSS lie mostly at the bluest $(g - r)$ colours.

We suggest a simple colour cut of $(g - i) = 2.35$ above which almost all (90 per cent) of our BOSS galaxies have an early-type morphology in both the LOZ and CMASS samples (numbers are given in Table 1). Even possibly dust-reddened inclined spirals are

---

[5] Colours include Galactic extinction corrections.
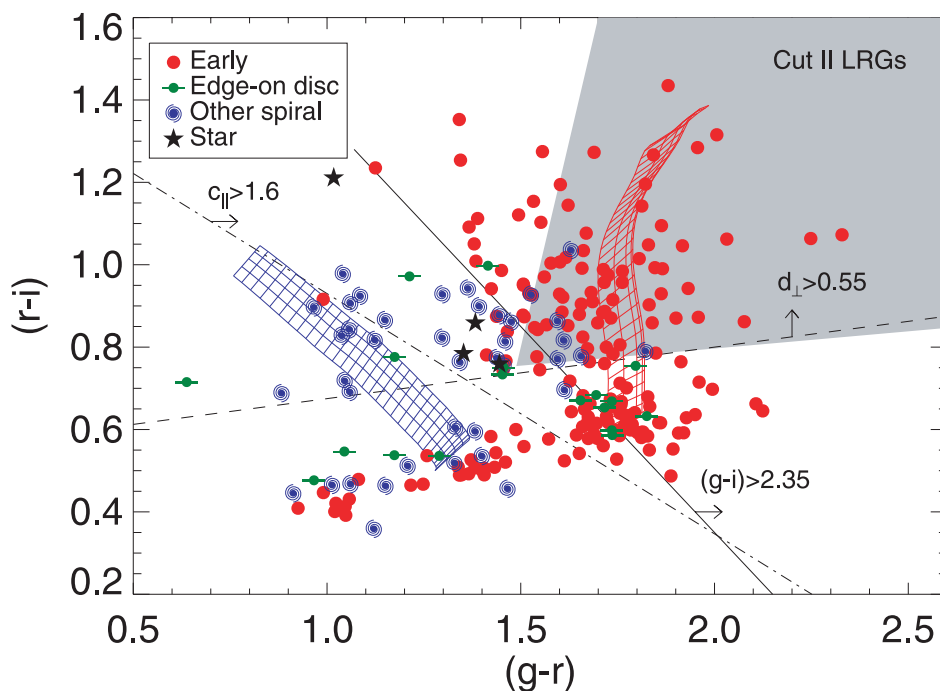
Figure 4. The $(g - r)$ versus $(r - i)$ colours for our sample of BOSS galaxies found in COSMOS *HST* imaging. The median photometric errors on these colours are $\sigma_{(r-i)} = 0.05$ and $\sigma_{(g-r)} = 0.11$. The dashed line shows the *gri* colour combination, $d_\perp > 0.55$ limit for the CMASS sample (CMASS objects lie above this line.). The solid black line illustrates a simple colour cut at $(g - i) = 2.35$ which can be used to remove most of the late-types in the BOSS sample. The dot–dashed line shows the *gri* colour combination, $c_\parallel > 1.6$ cut used by the 2 Degree Field and SDSS LRG and Quasar (2SLAQ) survey (Cannon et al. 2006) to define LRGs. The shaded region in the top-right corner of the plot shows the Cut II LRG sample from the original SDSS-I/II (Eisenstein et al. 2001). The red and blue grids show theoretical model tracks for passive LRGs (red) and constantly star-forming galaxies (blue) with $0.4 < z < 0.7$ (grid shows $\Delta z = 0.01$) and ages of 4, 5, 6, 7 and 8 Gyr.

rarely redder (in the optical) than this colour cut. For example, for the CMASS sample, 91 per cent of the early-type galaxies are redder than $(g - i) = 2.35$ while 76 per cent of the late-type galaxies are bluer than this cut.

The power of such a simple $(g - i)$ colour cut can be easily understood by looking at Fig. 4, where theoretical model tracks (from Maraston 2005 and Maraston et al. 2009) for different star formation histories, dust content and age are plotted in the observed frame for redshifts $0.4 < z < 0.7$. The age of the models, intended as the time after the start of star formation, is between 3 and 8 Gyr, which covers the age of the Universe adopting a galaxy formation redshift of $z = 5$. The red grid shows the LRG model of Maraston et al. (2009), which nicely covers the area where the CMASS early-types are found. The bluest late-types within CMASS [at $(g - r) \sim 1$ and $(r - i) \sim 0.8$] are well represented by a model with constant star formation ($\tau \sim 20$ Gyr) and a $E(B - V) = 0.3$ using a Calzetti et al. (2000) reddening law (blue grid).

We point out that at the CMASS redshifts, a $(g - i)$ observed-frame colour is almost equivalent to a $(u - r)$ rest-frame colour (the centre of *u* shifts to *g* at $z = 0.4$, while *r* shifts to *i* at $z > 0.2$). Our $(g - i) > 2.35$ colour separation can therefore be compared to $(u - r)$ colour selections in the local galaxy population, so we note that this cut is very similar to the optimal separator of $(u - r) = 2.22$ derived by Strateva et al. (2001) for the SDSS main galaxy sample (MGS), and to the similar $(u - r)$ cut derived as a function of M_r by Baldry et al. (2004) which asymptotes to roughly $(u - r) = 2.3$ for the most luminous galaxies.

Cannon et al. (2006) used a similar colour cut ($c_\parallel > 1.6$; which we show in Fig. 4 by a dot–dashed line) which was introduced to remove late-type galaxies in the 2SLAQ LRG sample. This colour

cut is often used in photometric redshift studies (e.g. Ross et al. 2011) as it has been empirically observed to help remove galaxies with unreliable photometric redshifts. As is clear in Fig. 4, our proposed colour cut is more efficient in removing late-type systems particularly in the CMASS galaxy sample.

We also show in Fig. 4 the Cut II LRG selection from SDSS-I/II (Eisenstein et al. 2001a) (shaded region). In the COSMOS area, 70 BOSS targets make this colour selection, with 91 per cent (64) of them being early-type galaxies. Note that the BOSS sample is deeper than the original Cut II LRG selection which had an average source density of 12 LRGs deg^{-2}. A total of only four original Cut II SDSS-I/II LRGs were observed in the COSMOS field. Finally, we remind the reader that the LOZ selection of BOSS (points with $d_\perp < 0.55$ in Fig. 4) is similar to (but deeper than) the SDSSI/II Cut I LRG sample. A total of 51 Cut I LRGs were observed in the COSMOS area.

In the following sections, we give more details on the various morphological sub-types.

3.2 Unresolved objects

We find four of the 240 BOSS targets which in the *HST* imaging are made up of unresolved point sources (stars or AGN). These objects passed the BOSS star–galaxy separation, but clearly have diffraction spikes in the COSMOS imaging. Two of the four point source systems are actually composed of two point sources each which are merged into single objects in BOSS imaging. We expect that the COSMOS field might have a lower stellar contamination rate than the rest of the survey because it was selected as a deep extragalactic field and is located away from the plane of our Galaxy

at a Galactic latitude of $b = 42°$. However, our visual inspection gives a point source contamination rate of 2 ± 1 per cent for BOSS targets which agrees, within the error, with the stellar contamination rate from the BOSS spectra taken to date, i.e. 3.38 per cent of BOSS spectra taken of targeted galaxies are stars (David Wake, private communication).

In addition, we look at objects in the COSMOS field which pass all BOSS target selection except the star–galaxy separation (which is based on the difference between PSF and model magnitudes in the SDSS pipeline). For the LOZ subset there are three such objects, all of which are point sources in the *HST* imaging. In the CMASS subset there are 18 such objects, four of which turn out to be galaxies (extended objects) in the *HST* imaging. This indicates that 3 ± 2 per cent (4/129) of CMASS galaxies or 2 ± 1 per cent (4/240) of all BOSS target galaxies in COSMOS are missed due to the star–galaxy separation, consistent with our expectation of <2 per cent for the whole survey.

3.3 Late-type galaxies

Of the late-type galaxies in the BOSS COSMOS sample (which make up 24 ± 3 per cent of all BOSS target galaxies), approximately a third are viewed edge-on (31 ± 8 per cent), by which we mean they show the classic Sp, or 'spindle' spiral type where no part of the face-on disc can be seen – we estimate this includes objects within about $5°–10°$ of completely edge-on. This value is larger than the fraction expected from random inclinations on the sky, where we would expect, for example, only 10 per cent of the systems should be within $5°$ of edge-on, or a quarter within $15°$ of edge-on.

Breaking the late-types into CMASS and LOZ sub-samples, we find that the bulk of this excess of edge-on discs is caused by the LOZ sub-sample, with the CMASS sample having an edge-on fraction consistent with random (6/34 objects, or 18 ± 7 per cent), while edge-on discs in the LOZ sample make up almost half of the late-types (12/25 objects, or 48 ± 14 per cent).

The high fraction of edge-on disc galaxies in the LOZ sub-sample suggests that something in the LOZ target selection is preferentially allowing in disc galaxies if they are seen in the edge-on orientation. Edge-on discs will be observed to both be redder (due to dust reddening) and have higher surface brightness and concentration than if seen face-on (e.g. Masters et al. 2010a). As we discuss above, the LOZ sub-sample is a fainter version of the SDSS I/II Cut I LRG selection (Eisenstein et al. 2011). Unlike the CMASS selection (which has a colour cut designed to select only on redshift) this LRG selection for LOZ has a cut on intrinsic colours which risks preferentially allowing in edge-on dust reddened discs. For example, there is a cluster of edge-on spirals at colours of $(g − r) > 1.7$ and $(r − i) \simeq 0.6$ in Fig. 4. We expect that surface brightness selection is not likely to be a big issue for BOSS late-type galaxies which are all massive spirals and as such should not even when seen face-on have low enough surface brightness to miss selection.

Overall, 8 ± 2 per cent of all BOSS targets studied here (5 ± 2 per cent of CMASS and 12 ± 3 per cent of LOZ) are highly inclined disc galaxies, and could represent a worrying contamination to the BOSS samples. For example, Yip et al. (2011) and Ross et al. (2011) have investigated inclination-dependent reddening as a source of systematic error for photometric redshift estimates. Also, since the intrinsic rest-frame colours of these edge-on disc galaxies are almost certainly bluer than their 'observed' rest-frame colours, and their luminosities are dimmed, their true stellar masses may be biased from estimated values. The amount and sense of this stellar mass bias depend on the details of the colours and luminosity used in a

stellar mass estimate (Maller et al. 2009). Usually, the stellar masses derived from full SED fitting of highly reddened galaxies with ongoing star formation are underestimated because of the age–dust degeneracy (Maraston et al. 2010). In some stellar mass estimates, the reddening and dimming can cancel out the effect on the stellar mass (e.g. in the case of the colour-dependent *M/L* relation provided by Bell & de Jong 2001 dust attenuation moves galaxies parallel to the relation), but the cancellation is often only partial (e.g. Reyes et al. 2011), so care still needs to be taken.

Reassuringly, for many applications which will use only the CMASS subset, e.g. Ross et al. (2011), most of the edge-on discs are not found in the CMASS cut. Moreover, note that no inclined disc galaxy is as red as the reddest early-type galaxies in our sample of BOSS galaxies (e.g. towards the top-right corner of Fig. 4). This result suggests that dust reddening, even if significant, is a smaller effect than the natural spread in optical colours of massive galaxies due to their stellar populations combined with redshift. A similar result was found at lower redshift for the SDSS-I/II Galaxy Zoo sample (see Masters et al. 2010a).

We find that some of the non-inclined late-type galaxies in BOSS are still as red as the early-type galaxies, i.e. 10 ± 4 per cent of the galaxies redder than our proposed $(g − i) = 2.35$ colour cut in the CMASS sample (see Section 3.1 for details) are non-inclined late-type galaxies. These may be the high-redshift counterparts of the passive, red spirals seen at lower redshifts in the SDSS MGS (Masters et al. 2010b). Red disc galaxies have already been identified in the COSMOS imaging, at approximately the same fraction; e.g. Bundy et al. (2010) found 15 per cent of red sequence objects had discs at $z \simeq 0.5$.

3.4 Pairs, multiples and disturbed systems

We observe that 23 ± 4 per cent of the BOSS early-type galaxies are multiple systems (i.e. have multiple bright spots) in the *HST* data, yet are unresolved in the SDSS imaging (we find 23 ± 5 per cent in both CMASS and LOZ early-type galaxy sub-samples). We show example images of 10 of the CMASS multiple systems in Fig. 5. Since these objects are blended in the SDSS images (which have a seeing disc of typical size 1.1 arcsec), the typical angular separation is around 1.1 arcsec.

Some of these multiple *early-type* galaxies may be ongoing ('dry') mergers (e.g. van Dokkum et al. 1999; Naab, Khochfar & Burkert 2006) as the colour and morphology of the sub-components are consistently red and elliptical in shape. However, only a small fraction of them (5/40) show clear evidence for interacting (having a disturbed morphology) whereas most show no evidence for tidal features and therefore could be projection effects. On the other hand, Bell et al. (2006) argue that even in a single-orbit *HST* image, the morphological signature of interactions will be weak, so we may not expect many of our multiple systems to appear disturbed even if they are truly interacting. In addition to the 40 close pairs, we find 21 of the early-type galaxies have a disturbed morphology, and a further six have clear dust lanes (which are often associated with former mergers; e.g. Kaviraj et al. 2011). Taken to the extreme, these findings may imply that up to 67 of the 178 early-type galaxies (38 ± 5 per cent) may show evidence for ongoing or recent interactions.

The multiple fraction is lower for late-type BOSS galaxies than for the early-types. In the CMASS (higher redshift) we find 15 ± 7 per cent late-type multiples (or 5/34 objects), while in the LOZ (lower redshift) sample there are only two multiples out of 25 late-type galaxy systems. Most of these late-type multiples (5/6 in
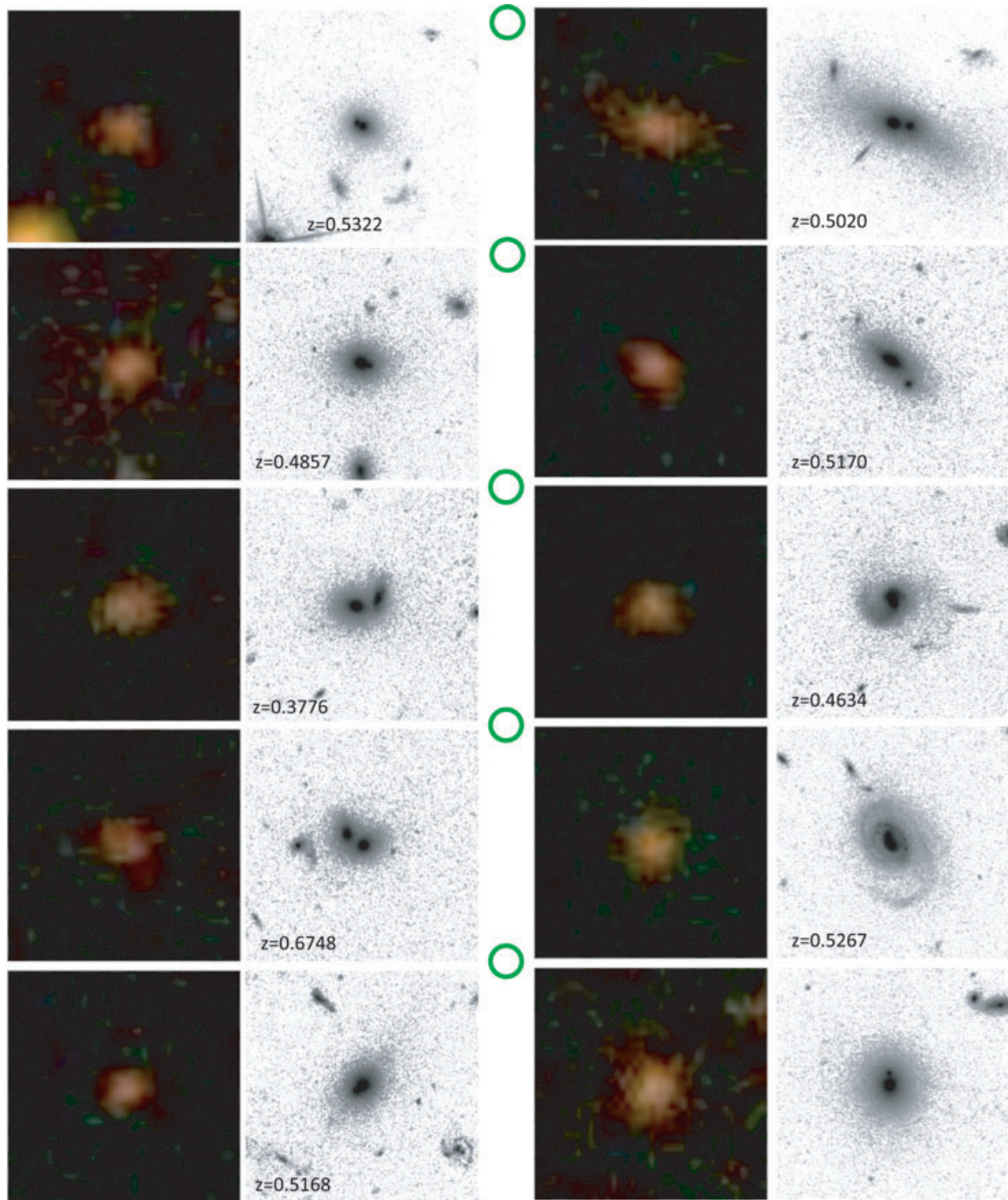
Figure 5. Similar to Figs 2 and 3, this shows examples of SDSS colour composite *gri* images, and ACS *I*-band images (black on white) for 10 of the BOSS CMASS galaxies which we find to have multiple components when observed at the higher *HST* resolution. All images are 15 arcsec^2, and the BOSS 2 arcsec diameter fibre is illustrated by the green circles. The multiple components are not always very clear at the contrast level shown here, but may be inspected in more details (and in the colour composite versions) at http://icg.port.ac.uk/~mastersk/BOSSmorphologies/. The redshifts of these galaxies from BOSS are indicated (no redshift is known for the bottom-right system).

total – note that one system satisfies both the CMASS and LOZ selection) also show a disturbed morphology; in addition we find five more late-type galaxies with evidence of a disturbed morphology.

We first investigate if these multiple systems are projection effects. This is can be estimated using the published angular correction function, $w(\theta)$, of the COSMOS galaxies by McCracken et al. (2007). They find $w(\theta) \simeq 1$ on scales of an arcsec, the typical seeing

of the BOSS data, for the brightest magnitude slice they considered ($21 < i_{AB} < 22$). This implies there are approximately twice as many observed pairs of galaxies in the COSMOS data at these small angular scales than expected from random associations, and there appears to be a steepening of the COSMOS correlation functions on these scales (see fig. 1 in McCracken et al. 2007). This estimate crudely agrees with the available *z*COSMOS spectroscopy (Lilly

et al. 2007) which provides redshifts for both components of two of our multiple systems (both early-types galaxies). One of these two multiple systems is a projection effect, while the other is a real association. A more detailed analysis of possible projection effects could be obtained from studying the angular clustering of COSMOS galaxies, with approximately the same colours and magnitudes as our BOSS galaxies, and/or studying the BOSS spectra for multiple redshifts (due to overlapping spectra from the components). Such analyses may become important in the future to fully understand all the systematic biases in the BOSS clustering measurements. For example, Le Fèvre et al. (2000) describe such a bias introduced into ground-based flux-limited samples (that lack the resolution to separate close pairs) which can cause merger-induced luminosity enhancements, i.e. the additional flux from a close companion can cause dimmer (or less massive) galaxies than desired to be added to the sample.

The separations of the components in the *HST* images are measured to go up to 2.0 arcsec, however this is for an object with worse than average SDSS seeing of 1.4 arcsec. A more typical separation for the majority of well-separated components is 1.2 arcsec. For the ≥ 50 per cent of multiples that are physically associated, we use this to derive a typical separation of 7.3 kpc assuming the mean CMASS redshift of $z = 0.5$. This value of projected separation suggests that the pairs lie within a single dark matter halo which would have a relatively short time-scale for merging (Rix & White 1989), perhaps less than half a gigayear (Bell et al. 2006). These physically associated multiple early-type BOSS galaxies will have merged into a single galaxy by $z = 0$ since $z = 0.5$ represents a lookback time of five gigayears.

Visual inspection suggests that up to half of the multiples could be major mergers (defined here as the components having flux ratios within the range of 1:4 of each other, and both components having similar optical colours). Unfortunately, the COSMOS pipeline photometry is likely to be unreliable for such close galaxy pairs which are not easily deblended, and a more quantitative analysis of the photometry of these multiples, to accurately measure their flux ratios and estimate their mass ratios and photometric redshifts, is beyond the scope of this paper. If approximately half of our multiples are indeed major mergers (and at least half are physically associated), this might appear to contradict the low rate of major mergers seen previously for massive galaxies (e.g. Le Fèvre et al. 2000; Masjedi et al. 2006; Jogee et al. 2009; Robaina et al. 2009; Bundy et al. 2009). However, we note that it has been argued that morphologically selected mergers (particularly in optical imaging) tend to be preferentially minor mergers (Bundy et al. 2004, 2010; Lotz et al. 2010), and also the range of major merger rates published for different samples with different colour and redshift is rather accommodating [see e.g. table 4 in Tojeiro & Percival (2010) which lists merger rates for massive galaxies from various samples of between 0.6 and 10 per cent per Gyr,[6] and also section 7 of Wake et al. (2008) which discusses the difficulty of performing such comparisons]. A more careful analysis will be required to properly derive the major merger rate but the relatively high fraction of unresolved multiples remains an interesting observation from our COSMOS sample of BOSS galaxies.

3.5 Comparison with ZEST types

The ZEST (Scarlata et al. 2007) uses a principal component analysis of five non-parametric measurements of a galaxy structure (asym-

---

[6] The full BOSS redshift range spans almost 4 Gyr.

metry, concentration, a measure of uniformity, the second order moment of bright pixels and the ellipticity) to assign basic morphological types to COSMOS galaxies. ZEST classifications are available for 231 of our BOSS targets (unresolved sources and targets near the edges of COSMOS images are not included). In the ZEST catalogue, types are parametrized by a morphological code ($T = 1$ for early-type galaxies, $T = 2$ for disc galaxies and $T = 3$ for irregulars), while for disc galaxies a 'bulginess' parameter is also given, ranging from $B=1$ for bulge-dominated galaxies to $B = 4$ for a pure disc galaxy.

Fig. 6 shows a comparison of the ZEST types with our visual classifications. On the *x*-axis is the SDSS $(g - i)$ colour, which we have shown to correlate with our visual types. We split the ZEST types along the *y*-axis into bins representing 'early' ($T = 1$), 'bulgy disc' ($T = 2$ and $B = 1$), 'intermediate disc' ($T = 2$ and $B = 2$ or 3), 'pure disc' ($T = 2$ and $B = 4$), 'irregular' ($T = 3$) and finally 'unclassified' ($T = 9$). We find a good overall agreement between ZEST and our visual classifications. For example, amongst the ZEST identified early-type galaxies in our sample, we identify 90 per cent (103/115) with the same morphology. Amongst the ZEST intermediate and pure disc galaxies, we identify 77 per cent (17/22) as having a disc (late-types or S0s).

Overall, we conclude that our visual identifications are in excellent agreement with those from the ZEST catalogue, i.e. up to 90 per cent of the time the two classifications agree, with the most uncertain galaxies being the early-type disc galaxies (lenticulars).

3.6 Shape and morphology: the axial ratio

We measure the shape of BOSS target galaxies in SDSS imaging by using the axial ratio, a/b, from the exponential model fit to the *i*-band data. We chose this rather than the de Vaucouleurs model fit, as only in disc galaxies should this quantity differ significantly from unity (round) when such objects are viewed nearly edge-on. We have checked the difference between the exponential and de Vaucouleurs fit measurements of the axial ratio and find it to be small [$\Delta \log (a/b) = -0.01 \pm 0.21$] with no obvious trend with visual morphology. We have also checked this value against the axial ratios from the GIM2D fits of ZEST and again find the difference to be small [$\Delta \log (a/b) = 0.01 \pm 0.09$].

In Fig. 7, we show all 240 BOSS objects in the COSMOS field as a function of visual morphology, colour and axial ratio [expressed as $\log (a/b)$]. We find that almost all our BOSS targets in the COSMOS field have an axial ratio of $a/b < 5$, or $\log (a/b) < 0.7$. The only objects with highly elongated shapes in our field (i.e. $a/b > 5$) are the two objects which turn out to be composed of pairs of point sources and which have $a/b = 20$ (not shown in the figure). This fact could be used to remove such binary point source contamination from the remaining BOSS galaxy targets.

For targets which are visually confirmed galaxies, the axial ratios behave as expected, with early-type galaxies being preferentially rounder and the most elongated galaxies being inclined spiral galaxies [see e.g. Alam & Ryden (2002), Padilla & Strauss (2008) for a discussion of the shape, colour and morphologies of the local galaxy population]. However, we point out that the rounding effects of seeing (e.g. as described in Masters, Giovanelli & Haynes 2003, and very obvious in the SDSS images shown in Figs 1 and 2) make even the most inclined BOSS late-types relatively round objects, so only qualitative comparison with local studies should be attempted.

The distribution of the axial ratios of our early-type galaxies is consistent with the findings of morphological studies performed with local galaxies. Early-types show a dichotomy with bright
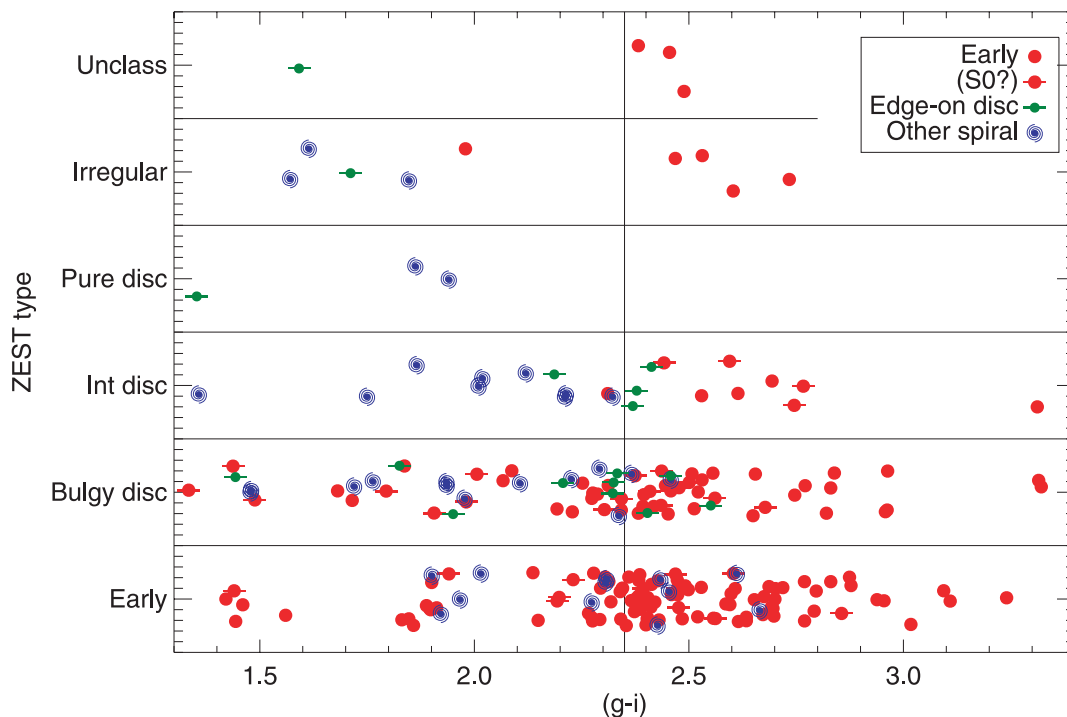
Figure 6. A comparison between our visual morphological types of BOSS galaxies and the automatically generated morphology in the ZEST catalogue (Scarlata et al. 2007). We split the ZEST types into 'early' ($T = 1$), 'bulgy disc' ($T = 2$, and $B = 1$), 'intermediate discs' ($T = 2$, and $B = 2$ or 3), 'pure disc' ($T = 2$ and $B = 4$), 'irregular' ($T = 3$) and 'unclassified' ($T = 9$). We have artificially scattered the data points in the y-direction within each category. Along the x-direction we plot the $(g - i)$ colour which we showed in Section 3.1 can be used to divide the galaxy population. The vertical solid line shows our $(g - i) = 2.35$ divider. The median error in this colour combination for the BOSS-COSMOS sample is $\sigma_{(g-i)} = 0.1$.
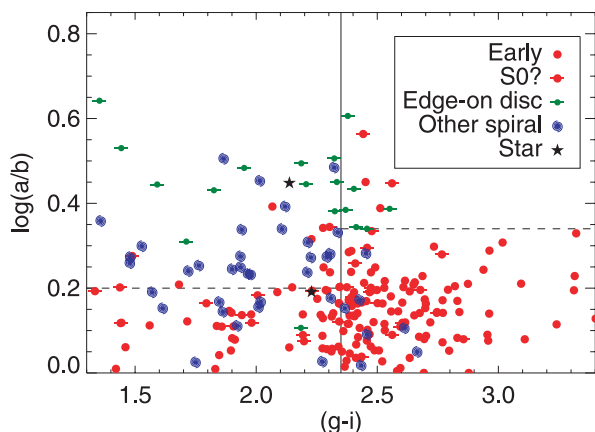
Figure 7. The $(g - i)$ colour versus axial ratio (from the *i*-band exponential fit) for the 240 BOSS targets with COSMOS imaging. The vertical line illustrates our suggested cut at $(g - i) = 2.35$, while the horizontal dashed lines are at $\log(a/b) = 0.2$ and $\log(a/b) = 0.34$, which remove most of the late-type BOSS galaxies and edge-on spirals.

ellipticals that are rounder while low-luminosity ellipticals and S0 can be flatter if viewed edge-on (Kormendy & Bender 1996). This classification has been confirmed and extended with the Spectrographic Areal Unit for research on Optical Nebulae (SAURON) sample (de Zeeuw et al. 2002) introducing a new parameter based on the angular momentum of the galaxy that separates early-types in slow and fast rotators (Emsellem et al. 2007; Cappellari et al. 2007). Slow rotators tend to be quite round while the fast rotators can be more flattened (again depending on viewing angle). This appears similar to Fig. 7, in which the bulk of early-types (mainly

bright E, i.e. slow rotators) have $\log(a/b) < 0.2$, but there are some with $\log(a/b) > 0.2$ that could correspond to the E-S0 SAURON fast rotators. Recent work on the morphology of nearby galaxies (Cappellari et al. 2011a,b; Emsellem et al. 2011) has confirmed the differences in the axial ratios described above using the much wider ATLAS3D sample (Cappellari et al. 2011a).

All the inclined spiral galaxies in our BOSS sample could be removed by requiring the SDSS axial ratio to be $\log(a/b) < 0.34$. The only exception is a galaxy near a bright star. This axial-ratio cut is particularly useful in the LOZ sample where, as illustrated in Fig. 4, the colour cut alone leaves a substantial number of edge-on late-type galaxies in the sample.

3.7 Redshift, luminosity and morphology

In Fig. 8, we show the BOSS targets with reliable redshifts in the COSMOS field versus a combination of *gri* photometry, $d_\perp = (r - i) - (g - r)/8.0$, which is used in the target selection (see Section 2.3). Symbols indicate the visual morphology. By design, this *gri* colour combination tracks the redshift of a passively evolved stellar population and a cut of $d_\perp > 0.55$ selects the higher redshift CMASS subset in BOSS (shown by a horizontal line in Fig. 8). It has already been demonstrated that this cut accurately isolates $z > 0.4$ galaxies in BOSS (White et al. 2011). We show here that this is true regardless of the visual morphology of the BOSS galaxies. We find that in this higher redshift subset, only two significantly lower redshift galaxy interlopers are present (or 0.8 ± 0.6 per cent of the resulting sample), both of which are inclined spiral galaxies which we suggest may be dust reddened into the selection of $d_\perp > 0.55$. It is interesting to notice that in fig. 1 of White et al. (2011), which shows the redshift distribution of the first semester of CMASS
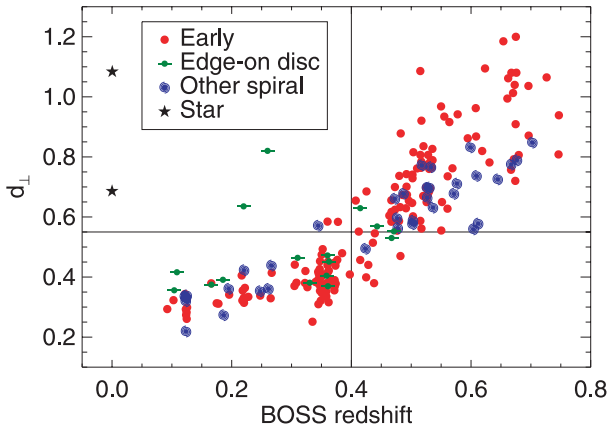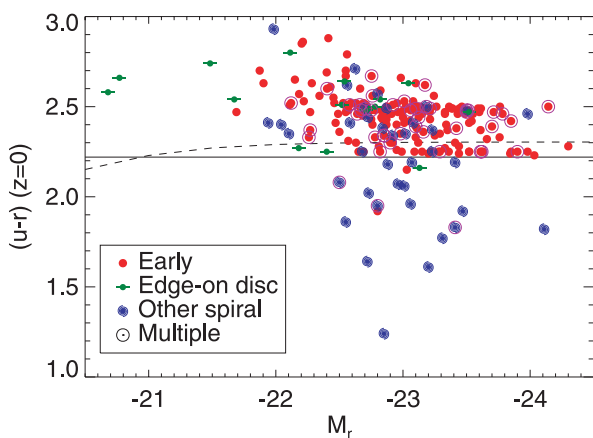
Figure 8. Redshifts of targets plotted against $d_\perp = (r - i) - ((g - r)/8)$ for the 224 targets with reliable redshifts in the COSMOS field. The horizontal line is $d_\perp = 0.55$ which is the selection used for the CMASS subset. The vertical line shows $z = 0.4$.

galaxies, there is a small bump present at $z \sim 0.2$ which we now suggest is probably explained by these inclined spiral interlopers into the CMASS colour selection.

We also point out in Fig. 8 the clear overdensity at $z = 0.35$ in the COSMOS field, which has previously been noticed (e.g. Kovač et al. 2010) and which clearly illustrates the well-known morphology–density relation.

In Fig. 9, we plot the rest-frame colour $(u - r)$ versus the observed-frame absolute magnitude (M_r) for the COSMOS BOSS galaxies with redshifts. The k-corrections are derived using fits to the mixed model of Maraston et al. (2006) where the galaxies have $(g - i)_{obs} < 2.35$ and to the LRG model of Maraston et al. (2009) otherwise. We show for comparison the colour dividers derived by Strateva et al. (2001; solid line) and Baldry et al. (2004; dashed line) for the local galaxy population. Most BOSS targets have (rest-frame) r-band absolute magnitudes above $M_r < -21.5$ and thus represent the high-luminosity end of the colour–magnitude (CM) relationship, where the main loci of the red sequence and blue cloud

Figure 9. The CM diagram showing $(u - r)$ and M_r k-corrected to $z = 0$ for BOSS galaxies in the COSMOS field with redshifts. The horizontal line shows $(u - r) = 2.22$ derived as an optimal separator for the $z = 0$ galaxy population by Strateva et al. (2001), while the dashed line is the similar magnitude-dependent separator derived by Baldry et al. (2004). Since BOSS targets only massive, luminous galaxies, they lie at the luminous end of the local CM where the main locus of the red sequence and blue cloud lie close together.

move close together in colour space. Nevertheless, we find that the BOSS late-type galaxies lie preferentially in the blue cloud. We point out that no internal extinction corrections have been applied for the disc galaxies – so the dust reddening may be significant (up to half a magnitude; Masters et al. 2010a) for the edge-on discs (green symbols). We also indicate in Fig. 9 if the galaxies are unresolved multiples, and therefore possibly merger events. Such objects have no obvious offset in this CM diagram, indicating there is no evidence for merger-induced star formation.

4 CATALOGUED SIZES OF BOSS GALAXIES

The sizes of massive galaxies at high redshifts have been a topic of significant interest in recent years (e.g. Trujillo et al. 2006; Cimatti et al. 2008; Mancini et al. 2009; Shankar & Bernardi 2009; van der Wel et al. 2009; Maltby et al. 2010), providing new constraints on hierarchical galaxy evolution models (e.g. Almeida, Baugh & Lacey 2007; Shankar et al. 2010, 2011). Many observations of massive galaxies at $z > 1$ suggest they are significantly more compact than their counterparts at $z = 0$ (e.g. Daddi et al. 2005; Trujillo et al. 2006; Longhetti et al. 2007; Cimatti et al. 2008; van Dokkum et al. 2008; van der Wel et al. 2008). This size evolution is in qualitative agreement with the models, but indicates stronger evolution than is usually predicted (although Mancini et al. 2009 have argued the observed size evolution may be overestimated due to the lower signal-to-noise ratio of high-redshift observations). These studies have largely focused on comparing high-redshift ($z > 1$) galaxies with the local galaxy population. The CMASS sample of BOSS, representing massive luminous galaxies at an intermediate-redshift range of $0.4 < z < 0.7$, will therefore be an important sample to link the two populations, and further test such models. Accurate size measurements for all BOSS galaxies, but particularly the CMASS subset, are therefore of significant interest, important not only for this test, but also for measuring accurate dynamical masses (see e.g. Beifiori et al., in preparation).

The median (seeing-corrected) effective radius of our sample of BOSS galaxies is 1.5 arcsec (1.2 arcsec for CMASS and 1.9 arcsec for LOZ), taken from the de Vaucouleurs fit to either the SDSS r-band or i-band images. This is close to the median seeing of the SDSS-III DR8 imaging (Section 2.2). In this section, we will compare the SDSS pipeline size measurements for CMASS galaxies to those measured from COSMOS imaging provided by ZEST (Scarlata et al. 2007). There are 129 CMASS targets in the COSMOS field, of which 123 have sizes reported in ZEST (the six with no reported size comprise the four shown to be made up of point sources in the *HST* imaging, and two galaxies which are near the edges of COSMOS *HST* images).

ZEST provides Sersic fits to the *HST* galaxy profiles using the GIM2D software (Sargent et al. 2007),[7] while the effective radii from the SDSS pipeline analysis are based on a de Vaucouleur fit, i.e. an $n = 4$ Sersic profile. Here, we present a simple comparison between the SDSS pipeline (de Vaucouleurs model) and ZEST (Sersic model) effective radii. While it is clear that if the true galaxy profile is a Sersic profile (i.e. with arbitrary n) then forcing it to an $n = 4$

---

[7] We use the parameter R_GIM2D from the ZEST fits, which we point out is the effective radius from the version of the Sersic profile in which this radius is defined to be identical to the half-light radius, i.e. $I(r) = I(0)\exp(-b_n(r/r_e)^{1/n})$, where the constant b_n is a function of the shape parameter, n, chosen such than $r_e = r_{1/2}$, and is well approximated by $b_n = 2n - 0.324$ for $1 < n < 15$ (Trujillo, Graham & Caon 2001).
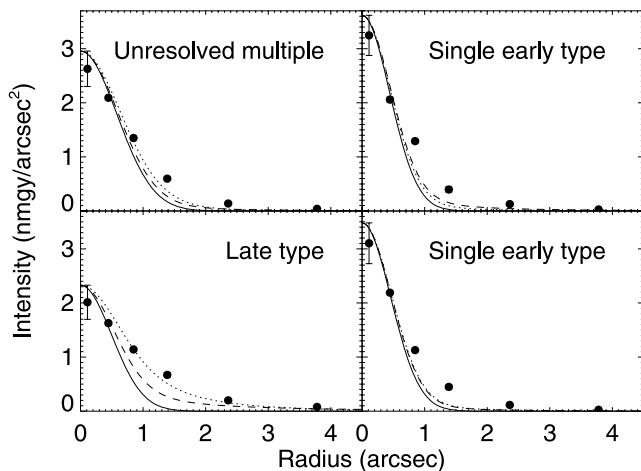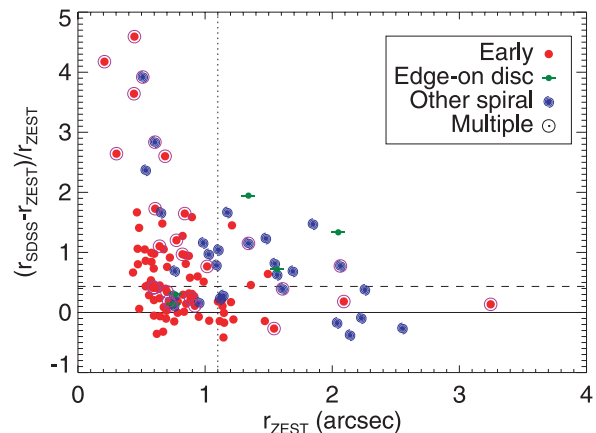
Figure 10. Example SDSS *i*-band profiles of four CMASS galaxies. Shown are a Gaussian PSF (solid line), the SDSS de Vaucouleurs fit (dashed line) and the ZEST Sersic fit (dotted line). The latter two models are convolved with a single Gaussian PSF. There is offset applied to all three model profiles such that they set to be equal to the maximum of the error range at $r = 0$.

Figure 11. Relative difference between the SDSS pipeline effective radius and the effective radius reported in ZEST as a function of the ZEST size. The median difference of 43 per cent is shown with the dashed line. Visual morphologies are indicated by the symbols as per the legend. Where two symbols overlap the galaxy is found in both categories (e.g. multiple early types).

profile while fitting will affect the estimate of the effective radius [e.g. see fig. 4 of Trujillo et al. (2001) which shows the analytic description of how this approach may change the effective radius when using ideal profiles with no seeing, or random noise], we argue that this effect is not likely to be the dominant bias on the effective radii of CMASS galaxies measured by SDSS. In this case, the seeing is comparable in size to the effective radius, so the profile shape fit is actually dominated by the point spread function, and furthermore is constrained by a small number of (five or six) data points. To illustrate this effect, we show in Fig. 10 four example profiles of BOSS galaxies compared to a Gaussian point spread function (solid line; we note that in SDSS the seeing disc is actually fit as a double Gaussian which would extend to even larger radii than the single Gaussian shown as a guide here), a de Vaucouleurs profile (dashed line) and a Sersic profile (dotted line).

The effect of seeing on the SDSS profiles is so significant that it is almost impossible to distinguish between the Sersic and de Vaucouleurs fits. As will be shown in Beifiori et al. (in preparation) it is not possible to fit Sersic profiles to the SDSS imaging data of galaxies at the redshifts of BOSS galaxies as there is not enough information to constrain both n and the effective radius, and in addition the strong correlation between n and r_e means that errors in the value of n will result in changes in the inferred value of r_e.

We show the relative difference between the SDSS pipeline and ZEST sizes as a function of the ZEST size in Fig. 11. We see no trends of the difference with the ZEST Sersic fit n, and the difference in effective radius between the two pipelines does not follow the theoretical expectation for best-fitting de Vaucouleurs values to a Sersic profile. We argue that this is further evidence that the dominant bias is not due to fitting an $r^{1/4}$ model in the SDSS images. The median relative difference between SDSS pipeline effective radii of CMASS targets (in i band) and those from ZEST fits is $+43 \pm 90$ per cent (i.e. SDSS sizes are on average 43 per cent larger) but the relative measurement difference ranges from -50 to $+500$ per cent. In absolute value, this full range corresponds to -0.8 to 2.7 arcsec, and the median absolute difference is $+0.31 \pm 0.67$ arcsec.

As might be expected, the most catastrophic errors in the SDSS sizes occur when the BOSS target is an unresolved multiple in the

SDSS imaging. In these cases the ZEST size measurement is of a single component, making it much smaller than the SDSS size which represents the separation of the multiple system. Almost all objects with relative differences greater than $+200$ per cent are unresolved multiples which have ZEST sizes $\simeq 0.5$ arcsec, but SDSS sizes >1.5 arcsec (see Fig. 11). Such objects cannot be removed using any cuts described above with SDSS data, and we have yet to find any alternative criterion based on SDSS data alone which can remove them.

There is no significant improvement in the median relative difference (i.e. it remains at $+40$ per cent) by removing blue [i.e. $(g - i) < 2.35$] or highly elongated [log $(a/b) > 0.34$] galaxies from CMASS. We also see no evidence for trends of the size difference with colour, morphology (either visual, or using the index of the ZEST Sersic fit, as discussed above), and also no trends with redshift. There are also no trends of the difference with the size of the SDSS seeing disc (which varies from 0.95 to 1.4 arcsec) in the COSMOS area. Also there are no correlations with the reported likelihood of the SDSS de Vaucouleurs fit, or the reported error on the SDSS effective radius.

One caveat here is that the BOSS target galaxies are very large galaxies for COSMOS. It has been shown that Sersic profile fits will underestimate effective radii in cases where the sky is marked too close to the galaxies (as first noted by Trujillo et al. 2001). It seems feasible that this could be a problem especially for the larger galaxies in COSMOS. We will present a much more comprehensive comparison of various size measurements of BOSS target galaxies considering issues like this further in a future paper (Beifiori et al., in preparation).

5 CONCLUSIONS

We present a study of the visual morphology and measured size of galaxies from the BOSS. We focus on a sample of BOSS galaxies that overlap with the COSMOS, which possess high-resolution, deep *HST* imaging data. Our major conclusions are as follows.

(i) We find that 76 ± 3 per cent of BOSS galaxies in both the 'CMASS' and 'LOZ' samples have an early-type visual morphology and the red colours typical of passive galaxies at the targeted redshift. This is in agreement with the modelling of the survey

target selection. The remainder of BOSS galaxies have a late-type morphology.

(ii) We show that a simple colour cut of $(g - i) = 2.35$ serves to remove most of the late-type galaxies in both the CMASS and LOZ sub-samples of BOSS galaxies, leaving each sample with ≥ 90 per cent early-type galaxies. We explain why this colour cut works using models, and point out that it is similar to the rest-frame colour cut of $(u - r) = 2.22$ derived for local galaxies (Strateva et al. 2001). Likewise, a simple cut of $\log(a/b) < 0.34$ on the axial ratio of BOSS galaxies would remove binary star systems and edge-on disc galaxies. Together, these cuts would produce as homogeneous sample of BOSS galaxies as presently possible, which may be required for some studies of galaxy evolution and cosmology.

(iii) We find more edge-on late-type galaxies in the LOZ subset than expected from random orientations on the sky, suggesting that this selection contains a sub-sample of inclined spirals preferentially making the sample selection. This problem may become a major systematic effect for detailed studies of the BOSS sample, e.g. photometric redshift estimations (see Yip et al. 2011; Ross et al. 2011). The colours of these inclined spirals are, however, still not as red as the reddest early-type galaxies in our sample, indicating that the colours of BOSS galaxies are dominated by their redshift and stellar populations.

(iv) We find intrinsically red spiral galaxies (i.e. not highly inclined), which may be analogous to the 'passive red spirals' found recently in both the local Galaxy Zoo data set (Masters et al. 2010b) and in the COSMOS field (Bundy et al. 2010). These objects make up 10 ± 3 per cent of the galaxies in the sample with $(g - i) > 2.35$.

(v) For the early-type BOSS galaxies, we find a significant fraction (23 ± 4 per cent) are unresolved multiples in the SDSS imaging. We estimate that at least 50 per cent of these multiples are likely real associations and not projection effects. For those which are physically associated, the components of these multiple system are relatively close (~ 7 kpc at the median redshift of BOSS), and we conclude that many are likely on-going 'dry mergers' that reside in the same dark matter halo and will merge completely on a short time-scale (Bell et al. 2006).

(vi) The standard SDSS pipeline measurements of sizes for BOSS galaxies have a median size of 1.5 arcsec (1.2 arcsec for CMASS and 1.9 arcsec for LOZ), meaning that the bulk of BOSS galaxies are barely resolved in the SDSS imaging. SDSS measurements of the seeing-corrected effective radius of CMASS galaxies are on average 0.3 arcsec (40 per cent) larger than similar measurements made from the *HST* imaging (using the ZEST catalogue of Scarlata et al. 2007) but show no trend with colour, morphology or redshift. A correction of -0.31 ± 0.67 arcsec can be applied to statistically correct the SDSS pipeline size measurements to make them agree with those from the *HST* imaging (but there will still be significant error on an individual galaxy).

In this paper, we have demonstrated the effectiveness of the SDSS-III BOSS target selection which was aimed at selecting massive, luminous galaxies regardless of their morphology or star formation history. Most such galaxies are early-type and passive galaxies, but there exists a significant fraction of massive late-type galaxies. As shown in Figs 8 and 9, BOSS galaxies are predominantly passive, early-type, massive galaxies over the redshift range $0.1 < z < 0.7$. Approximately a quarter of BOSS galaxies are late-types. Depending on the science application, this subset of galaxies could represent a potential systematic uncertainty. The results of this paper will help users of the BOSS data to fine-tune their selections to obtain the sample of galaxies they require.

REFERENCES

Aihara H. et al., 2011, ApJS, 193, 29
Alam S. M. K., Ryden B. S., 2002, ApJ, 570, 610
Almeida C., Baugh C. M., Lacey C. G., 2007, MNRAS, 376, 1711
Baldry I. K., Glazebrook K., Brinkmann J., Ivezić Ž., Lupton R. H., Nichol R. C., Szalay A. S., 2004, ApJ, 600, 681
Ball N. M., Loveday J., Brunner R. J., 2008, MNRAS, 383, 907
Bamford S. P. et al., 2009, MNRAS, 393, 1324
Bell E. F., de Jong R. S., 2001, ApJ, 550, 212
Bell E. F. et al., 2006, ApJ, 640, 241
Blanton M. R., Eisenstein D., Hogg D. W., Schlegel D. J., Brinkmann J., 2005, ApJ, 629, 143
Bundy K., Fukugita M., Ellis R. S., Kodama T., Conselice C. J., 2004, ApJ, 601, L123
Bundy K., Fukugita M., Ellis R. S., Targett T. A., Belli S., Kodama T., 2009, ApJ, 697, 1369
Bundy K. et al., 2010, ApJ, 719, 1969

Calzetti D., Armus L., Bohlin R. C., Kinney A. L., Koornneef J., Storchi-Bergmann T., 2000, ApJ, 533, 682
Cameron E., 2011, PASA, 28, 128
Cannon R. et al., 2006, MNRAS, 372, 425
Cappellari M. et al., 2007, MNRAS, 379, 418
Cappellari M. et al., 2011a, MNRAS, 413, 813
Cappellari M. et al., 2011b, MNRAS, preprint (arXiv:1104.3545)
Cimatti A. et al., 2008, A&A, 482, 21
Daddi E. et al., 2005, ApJ, 626, 680
de Zeeuw P. T. et al., 2002, MNRAS, 329, 513
Dressler A., 1980, ApJ, 236, 351
Eisenstein D. J. et al., 2001, AJ, 122, 2267
Eisenstein D. J. et al., 2011, AJ, 142, 72
Emsellem E. et al., 2007, MNRAS, 379, 401
Emsellem E. et al., 2011, MNRAS, 414, 888
Fukugita M., Ichikawa T., Gunn J. E., Doi M., Shimasaku K., Schneider D. P., 1996, AJ, 111, 1748
Gunn J. E. et al., 1998, AJ, 116, 3040
Gunn J. E. et al., 2006, AJ, 131, 2332
Hogg D. W. et al., 2003, ApJ, 585, L5
Jogee S. et al., 2009, ApJ, 697, 1971
Kannappan S. J., Guie J. M., Baker A. J., 2009, AJ, 138, 579
Kauffmann G., White S. D. M., Guiderdoni B., 1993, MNRAS, 264, 201
Kaviraj S., Tan K.-M., Ellis R. S., Silk J., 2011, MNRAS, 411, 2148
Koekemoer A. M. et al., 2007, ApJS, 172, 196
Komatsu E. et al., 2011, ApJS, 192, 18
Kormendy J., Bender R., 1996, ApJ, 464, L119
Kovač K. et al., 2010, ApJ, 708, 505
Le Fèvre O. et al., 2000, MNRAS, 311, 565
Leauthaud A. et al., 2007, ApJS, 172, 219
Lilly S. J. et al., 2007, ApJS, 172, 70
Lintott C. J. et al., 2008, MNRAS, 389, 1179
Lintott C. J. et al., 2011, MNRAS, 410, 166
Longhetti M. et al., 2007, MNRAS, 374, 614
Lotz J. M., Jonsson P., Cox T. J., Primack J. R., 2010, MNRAS, 404, 575
McCracken H. J. et al., 2007, ApJS, 172, 314
Maller A. H., Berlind A. A., Blanton M. R., Hogg D. W., 2009, ApJ, 691, 394
Maltby D. T. et al., 2010, MNRAS, 402, 282
Mancini C., Matute I., Cimatti A., Daddi E., Dickinson M., Rodighiero G., Bolzonella M., Pozzetti L., 2009, A&A, 500, 705
Maraston C., 2005, MNRAS, 362, 799
Maraston C., Daddi E., Renzini A., Cimatti A., Dickinson M., Papovich C., Pasquali A., Pirzkal N., 2006, ApJ, 652, 85
Maraston C., Strömbäck G., Thomas D., Wake D. A., Nichol R. C., 2009, MNRAS, 394, L107
Maraston C., Pforr J., Renzini A., Daddi E., Dickinson M., Cimatti A., Tonini C., 2010, MNRAS, 407, 830
Masjedi M. et al., 2006, ApJ, 644, 54
Masters K. L., Giovanelli R., Haynes M. P., 2003, AJ, 126, 158
Masters K. L. et al., 2010a, MNRAS, 404, 792
Masters K. L. et al., 2010b, MNRAS, 405, 783
Naab T., Khochfar S., Burkert A., 2006, ApJ, 636, L81
Padilla N. D., Strauss M. A., 2008, MNRAS, 388, 1321
Reyes R., Mandelbaum R., Gunn J. E., Pizagno J., Lackner C. N., 2011, MNRAS, submitted (arXiv:1106.1650)
Rix H.-W. R., White S. D. M., 1989, MNRAS, 240, 941
Robaina A. R. et al., 2009, ApJ, 704, 324
Ross A. J., Brunner R. J., 2009, MNRAS, 399, 878

Ross A. J. et al., 2011, MNRAS, in press (astroph/1105.2320)
Sargent M. T. et al., 2007, ApJS, 172, 434
Scarlata C. et al., 2007, ApJS, 172, 406
Schawinski K., Thomas D., Sarzi M., Maraston C., Kaviraj S., Joo S.-J., Yi S. K., Silk J., 2007, MNRAS, 382, 1415
Schawinski K. et al., 2009, MNRAS, 396, 818
Schlegel D. J., Finkbeiner D. P., Davis M., 1998, ApJ, 500, 525
Scoville N. et al., 2007, ApJS, 172, 38
Shankar F., Bernardi M., 2009, MNRAS, 396, L76
Shankar F., Marulli F., Bernardi M., Boylan-Kolchin M., Dai X., Khochfar S., 2010, MNRAS, 405, 948
Shankar F., Marulli F., Bernardi M., Mei S., Meert A., Vikram V., 2011, MNRAS, submitted (arXiv:1105.6043)
Skibba R. A. et al., 2009, MNRAS, 399, 966
Stoughton C. et al., 2002, AJ, 123, 485
Strateva I. et al., 2001, AJ, 122, 1861
Thomas D., Maraston C., Schawinski K., Sarzi M., Silk J., 2010, MNRAS, 404, 1775
Tojeiro R., Percival W. J., 2010, MNRAS, 405, 2534
Trujillo I., Graham A., Caon N., 2001, MNRAS, 326, 869
Trujillo I. et al., 2006, MNRAS, 373, L36
van der Wel A., Holden B. P., Zirm A. W., Franx M., Rettura A., Illingworth G. D., Ford H. C., 2008, ApJ, 688, 48
van der Wel A., Bell E. F., van den Bosch F. C., Gallazzi A., Rix H.-W., 2009, ApJ, 698, 1232
van Dokkum P. G., Franx M., Fabricant D., Kelson D. D., Illingworth G. D., 1999, ApJ, 520, L95
van Dokkum P. G. et al., 2008, ApJ, 677, L5
Wake D. A. et al., 2008, MNRAS, 387, 1045
White M. et al., 2011, ApJ, 728, 126
Wolf C. et al., 2009, MNRAS, 393, 1302
Yip C.-W., Szalay A. S., Carliles S., Budavari T., 2011, ApJ, 730, 54
York D. G. et al., 2000, AJ, 120, 1579
Zehavi I. et al., 2005, ApJ, 630, 1

APPENDIX A: DATA TABLE

We provide here a sample of the basic data available on our sample of 240 BOSS galaxies. We list the equatorial coordinates of the galaxy (RA and Dec. in J2000), $(g - i)$ colour, redshift and (where available) the BOSS sub-sample for the galaxy (see Section 2.3) and the visual morphological type we assign (see Section 3). A page of the table (in which galaxies are presented in order of increasing RA) is shown below to illustrate the format. The full table is available electronically (see Supporting Information).

SUPPORTING INFORMATION

Additional Supporting Information may be found in the online version of this article:

Table A1. The BOSS-COSMOS cross match sample.

Please note: Wiley-Blackwell are not responsible for the content or functionality of any supporting materials supplied by the authors. Any queries (other than missing material) should be directed to the corresponding author for the article.

Table A1. The BOSS-COSMOS cross match sample. (The full table is available in the online version of the paper – see Supporting Information.)

RA (J2000 deg)	Dec. (J2000 deg)	$(g - i)$	Redshift	Redshift source	BOSS sub-sample	Visual type
149.45591	2.56332	2.69	0.3732	BOSS	LOZ	Early
149.46232	2.00290	2.23	0.3776	BOSS	CMASS	Early disturbed multiple
149.46780	2.67181	2.42	0.4284	BOSS	LOZ	Early
149.47437	1.97636	2.23	0.0004	BOSS	CMASS	Star
149.47484	1.95824	1.59	0.1084	SDSS2	LOZ	Late edge
149.47913	2.56491	2.43	0.3717	SDSS2	LOZ	Early
149.48440	2.39573	2.68	0.4819	BOSS	LOZ	Early
149.48441	2.43524	2.72	0.4800	BOSS	CMASS	Early
149.48569	1.81567	2.70	0.5301	BOSS	CMASS	Early
149.49280	2.15313	1.49	0.1254	SDSS2	LOZ	Early S0
149.49475	1.70034	1.94	0.5714	BOSS	CMASS	Late
149.49892	1.77765	1.76	0.5030	BOSS	CMASS	Late bar disturbed
149.50357	2.02399	2.53	0.6739	BOSS	CMASS	Early multiple
149.50510	1.93552	2.82	0.5356	BOSS	CMASS	Early multiple
149.52362	1.75892	2.84	0.5688	BOSS	CMASS	Early
149.52782	1.93026	2.70	0.5354	BOSS	CMASS	Early multiple
149.53110	2.44029	2.60	0.4960	BOSS	CMASS	Early disturbed
149.53903	1.72237	2.56	0.5016	BOSS	CMASS	Early
149.55600	2.52001	2.53	0.4857	BOSS	CMASS	Early multiple
149.57499	2.40669	2.43	0.4825	BOSS	CMASS	Early
149.58221	2.83479	2.35	0.3485	BOSS	LOZ	Early multiple
149.60008	2.82114	2.40	0.3446	SDSS2	LOZ	Early
149.60469	2.45263	2.01	0.6768	BOSS	CMASS	Late
149.61937	1.73545	2.96	0.5947	BOSS	CMASS	Early
149.61972	2.25936	2.52	0.3602	BOSS	CMASS	Early
149.63300	2.79217	2.29	0.4123	BOSS	CMASS	Early
149.63728	2.60176	3.02	0.5499	BOSS	CMASS	Early
149.63763	1.87079	2.37	–	No redshift	CMASS	Late bar
149.64264	2.47120	2.32	0.5264	BOSS	CMASS	Late
149.64834	2.81872	2.43	0.3446	SDSS2	CMASS and LOZ	Late bar disturbed multiple
149.65295	1.65853	2.55	0.4672	BOSS	LOZ	Late edge
149.65426	2.85348	2.02	0.7026	BOSS	CMASS	Late disturbed
149.66390	1.62584	2.38	0.4668	BOSS	CMASS	Early
149.68306	1.88888	2.53	0.5322	BOSS	CMASS	Early multiple
149.68626	2.33281	2.39	0.5515	BOSS	CMASS	Early
149.68789	2.65381	2.79	–	No redshift	CMASS	Early
149.68793	2.47519	2.44	–	No redshift	CMASS	Early bar S0 disturbed
149.68883	2.49744	2.34	0.4873	BOSS	CMASS	Late bar
149.69039	1.61994	2.77	0.4815	BOSS	CMASS	Early
149.69557	2.40576	4.04	0.6757	BOSS	CMASS	Early
149.70085	2.66303	2.67	0.4921	BOSS	CMASS	Early
149.70565	2.50560	2.70	0.4913	BOSS	CMASS	Early
149.71041	2.12273	2.56	0.4796	BOSS	CMASS	Early S0
149.71245	2.54465	2.63	0.4766	BOSS	CMASS	Early
149.71374	2.01956	2.29	0.6446	BOSS	CMASS	Late disturbed multiple
149.71858	1.63799	1.97	0.6671	BOSS	CMASS	Late disturbed
149.72159	1.73891	2.80	0.6606	BOSS	CMASS	Early disturbed
149.72647	2.41945	1.44	0.1248	SDSS2	LOZ	Early S0
149.72909	1.91729	2.30	0.3622	BOSS	LOZ	Early
149.73561	2.10550	2.37	0.5164	BOSS	CMASS	Early
149.73964	1.79295	1.86	-	No redshift	CMASS	Late bar
149.74285	2.17959	3.40	0.6308	BOSS	CMASS	Early multiple
149.75634	2.79470	2.73	0.4930	SDSS2	CMASS	Early multiple
149.76710	1.96770	2.61	0.5281	BOSS	CMASS	Early
149.77077	2.78284	2.46	0.5099	BOSS	CMASS	Early
149.77704	2.75691	2.29	0.3456	BOSS	LOZ	Early
149.77779	2.26297	2.02	q 0.4730	BOSS	CMASS	Late multiple
149.78498	2.53039	2.56	-	No redshift	CMASS	Early S0
149.79785	1.70203	2.34	0.3503	BOSS	LOZ	Early S0 disturbed
149.79810	1.80106	2.96	0.6621	BOSS	CMASS	Early
149.79882	1.97809	2.47	0.5257	BOSS	CMASS	Early S0 disturbed
..	..	..	..	..	..	

This paper has been typeset from a TeX/LaTeX file prepared by the author.